Temperature Responsive Hydrogel for Cells Encapsulation Based on Graphene Oxide Reinforced poly(N-isopropylacrylamide)/Hydroxyethyl-Chitosan

Lei Nie, Jie Li, Guoqi Lu, Xiaoyan Wei, Yaling Deng, Shuang Liu, Shengping Zhong, Qimin Shi, Ruixia Hou, Yi Sun, Constantinus Politis, Lihong Fan, Oseweuba Valentine Okoro, Amin Shavandi

PII: S2352-4928(22)00558-X

DOI: https://doi.org/10.1016/j.mtcomm.2022.103697

Reference: MTCOMM103697

To appear in: *Materials Today Communications*

Received date: 16 August 2021
Revised date: 19 April 2022
Accepted date: 16 May 2022

Please cite this article as: Lei Nie, Jie Li, Guoqi Lu, Xiaoyan Wei, Yaling Deng, Shuang Liu, Shengping Zhong, Qimin Shi, Ruixia Hou, Yi Sun, Constantinus Politis, Lihong Fan, Oseweuba Valentine Okoro and Amin Shavandi, Temperature Responsive Hydrogel for Cells Encapsulation Based on Graphene Oxide Reinforced poly(N- isopropylacrylamide)/Hydroxyethyl-Chitosan, *Materials Today Communications,* (2021) doi:https://doi.org/10.1016/j.mtcomm.2022.103697

Temperature Responsive Hydrogel for Cells Encapsulation Based on Graphene Oxide Reinforced poly(N- isopropylacrylamide)/Hydroxyethyl-Chitosan

Lei Nie[a,b,c,h,*], Jie Li[a], Guoqi Lu[a], Xiaoyan Wei[d], Yaling Deng[e], Shuang Liu[f], Shengping Zhong[b,c], Qimin Shi[b,c], Ruixia Hou[g], Yi Sun[b], Constantinus Politis[b], Lihong Fan[f], Oseweuba Valentine Okoro[h], and Amin Shavandi[h,*]

[a] College of Life Sciences, Xinyang Normal University, Xinyang 464000, China.

[b] Department of Imaging & Pathology, University of Leuven and Oral & Maxillofacial Surgery, University Hospitals Leuven, Leuven 3001, Belgium.

[c] Additive Manufacturing Research Group, Department of Mechanical Engineering, Katholieke Universiteit Leuven (KU Leuven) & Member of Flanders Make, Celestijnenlaan 300B, Heverlee 3001, Belgium.

[d] Department of Medicine, Division of Endocrinology, Diabetes and Metabolism, Johns Hopkins University School of Medicine, 600 Fifth Street S., 4th floor, Rm. 4402, St. Petersburg, FL 33701, USA

[e] College of Intelligent Science and Control Engineering, Jinling Institute of Technology, Nanjing 211169, P.R. China.

[f] School of Resources and Environmental Engineering, Wuhan University of Technology, Wuhan 430070, P. R. China

[g] Medical School of Ningbo University, Ningbo 315211, P. R. China

[h] Université libre de Bruxelles (ULB), École polytechnique de Bruxelles, 3BIO-BioMatter, Avenue F.D. Roosevelt, 50 - CP 165/61, 1050 Brussels, Belgium.

* Corresponding author I: Lei Nie

Post address: College of Life Sciences, Xinyang Normal University (XYNU), Xinyang 464000, China. Tel: +86-13600621068. ORCID: 0000-0002-6175-5883

E-mail address: nieleifu@yahoo.com; nielei@xynu.edu.cn

* Corresponding author II: Amin Shavandi

Post address: BioMatter unit - École polytechnique de Bruxelles, Université Libre de Bruxelles, Avenue F.D. Roosevelt, 50 - CP 165/61, 1050 Brussels, Belgium

E-mail address: amin.shavandi@ulb.be

Abstract:

Temperature-responsive hydrogels exhibit great potentials to encapsulate cells for 3D bioprinting and tissue engineering applications; however, cell aggregation and the hydrogel stiffness determine cell fate and limit its application. Here, we developed a new temperature-responsive hydrogel with interpenetrating polymer networks using poly (N-isopropylacrylamide) (pNiPAM) and hydroxyethyl-chitosan (HECS) with the incorporation of dithiol-modified graphene oxide nanosheets (t-GO). The fabricated hydrogel showed excellent cytocompatibility toward human bone marrow mesenchymal stem cells (hBMSCs), and as expected, the lower critical solution temperature (LCST) could be regulated by changing the weight ratio of pNiPAM/HECS/t-GO. Finally, hBMSCs could be directly encapsulated in the

hydrogel at a low temperature (around 20 °C), after then, the cell-laden hydrogel was formed above LCST and displayed high cell viability after 3D culturing. The results indicate that the new pNiPAM/HECS/t-GO hydrogel has the potential to serve as a cell carrier for drug delivery and tissue engineering applications.

Keywords: Temperature-responsive hydrogels; Cell encapsulation; Cytocompatibility; 3D microenvironment; Graphene oxide.

1. Intruduction

Tissue engineering combines scaffolds, cells, and growth factors to develop functional tissues could replace damaged or diseased tissues and organs [1,2]. Bio-functional scaffold should mimic at least partially the function of native tissue to transport cells to the damaged tissue [3]. Hydrogels are three-dimensional (3D) polymeric networks formed by a hydrophilic polymer that can retain a high amount of water and have tunable physical and chemical properties [4-7]. Significantly, the stimuli-responsive hydrogels can be reversibly transformed from sol to gel in response to temperature, pH, light, magnetic fields, ion strength, *etc.*, and the stimuli-responsive hydrogels have been studied for drug delivery, cell separation, tissue regeneration, and wound healing [8-20]. Poly(N-isopropylacrylamide) (pNiPAM) as a temperature-responsive polymer possesses an obvious coil-globule volume phase transition temperature (VPTT) of approximately 32 °C in water. The lower critical solution temperature (LCST) of pNiPAM can be fine-tuned close to human body

temperature by incorporating other hydrophilic or hydrophobic polymers, such as acrylic acid (AAc) and (meth)acrylamide derivatives of cholic acid [21,22].

The low polymer density in swollen states causes poor mechanical performance for native pNiPAM hydrogels, limiting their biomedical applications [23]. Such poor mechanical property could be overcame using multi-component hydrogels, and the analogous *in vivo* microenvironment could be provided, which are preferable for 3D scaffolds allowing cells to grow and maintain the original morphology and functionality [24-27]. Moreover, the stiffness of the hydrogel is the critical parameter that determines the cell fate, such as stem cells and cancer cells [28-30]. Interpenetrating polymer network (IPN) strategy has been widely reported to show tremendous enhancement of strength and toughness of hydrogels invariably, and such approach is sensible to be a preferable way for designing multi-component and multi-functional hydrogels [31-34].

Chitosan (CS) has attracted much attention due to its biocompatibility, low immunogenicity, and biological activities[35-37]. Introducing stimuli-responsive moiety into CS polymer network could design corresponding CS-based stimuli-responsive hydrogels[38,39]. For example, Wang *et al.* [40] grafted pNiPAM into CS backbone, and Ding *et al.* [41] synthesized pNiPAM/CS hydrogel via thiol-ene click chemistry, and the designed pNiPAM/CS hydrogel displayed thermos-responsive property. Hydroxyethyl-chitosan (HECS) is water-soluble due to the introduction of the hydroxyethyl group [42], and it is also biocompatible and biodegradable *in vivo* [43-45]. Nie *et al.* [46] reported a temperature-responsive hydrogel consisting of pNiPAM, CS, and

graphene oxide (GO), which was suitable for vascular endothelial cells (VECs) encapsulation and growth factor (GF) loading. However, the cell viability and the mechanical integrity of hydrogels limit its further potential application, such as 3D bioprinting. The GO nanosheets, as the polymer reinforcement, can endow composite materials with high strength and superior ductility [47,48], but the aggregation of GO nanosheets in polymer solution can cause the decrease of cytocompatibility of hydrogels. Such aggregation could be improved by grafting some molecules, such as *DL*-dithiothreitol (DTT), the dispersion of GO nanosheets in a polymer network could be also ameliorated, and the related properties could be further improved [49,50].

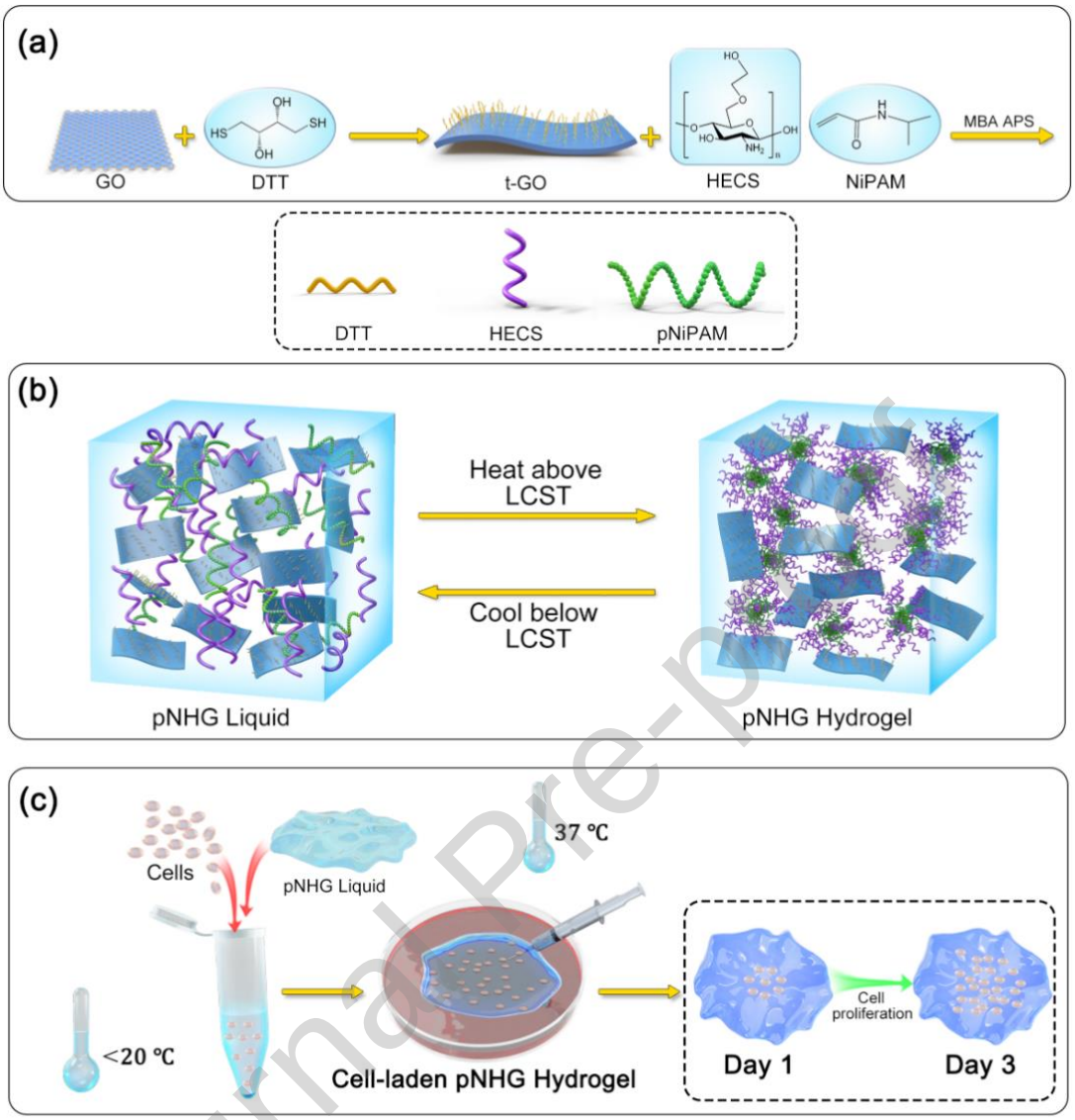

Figure 1. Schematic illustration of the synthesis of cell-laden pNiPAM/HECS/t-GO (pNHG) hydrogels. (a) Graphene oxide (GO) was modified by *DL*-dithiothreitol (DTT) to obtain t-GO nanosheets, then t-GO nanosheets were dispersed in pNiPAM/HECS (pNH) polymer network, (b) the pNHG hydrogel with interpenetrating networks could be formed increasing the temperature above LCST due to the interaction between the pNiPAM, HECS, and t-GO nanosheets, and the gelation mechanism was displayed. Next, (c) human bone mesenchymal stem cells (hBMSCs) were encapsulated into pNHG liquid at a lower temperature, after the sol-gel transfer with the increase of temperature, the cell-laden pNHG hydrogel was obtained for further 3D cell culture.

In the present study, for the first time, we report DTT-modified GO nanosheets (t-GO) reinforced temperature-responsive pNiPAM/HECS nanocomposite hydrogels (pNHG) with interpenetrating polymer networks for cells encapsulation, as shown in **Figure 1**. First, GO was modified using DTT molecules to obtain t-GO nanosheets. Then, t-GO, as a multifunctional crosslinker, was incorporated into pNiPAM/HECS polymer network to obtain pNHG hydrogel. The solubility of the pNHG nanocomposite in water was greatly improved compared with pNiPAM/HECS/GO nanocomposite[46], and t-GO can further reinforced the mechanical performance of pNHG hydrogel. Moreover, the sol-gel transfer temperature of pNHG hydrogels could be adjusted close to body temperature via regulating the weight ratio of pNiPAM/HECS/t-GO. Therein, the human bone mesenchymal stem cells (hBMSCs) have been successfully encapsulated in the hydrogels during the sol-gel transform process and displayed excellent viability after the 3D cell culture.

2. Materials and methods

2.1 Materials

N-Isopropylacrylamide (NiPAM, 98%), N, N'-Methylenebisacrylamide (MBA, AR), Ammonium Persulfate (APS, 98%), Sodium Bisulfite (SBS, AR) and *DL*-Dithiothreitol (DTT) were purchased from Shanghai Macklin Biochemical Co., Ltd. Graphite was purchased from Qingdao Henglide graphite Co. Ltd., Sodium nitrate ($NaNO_3$, ACS, 99.0%) and potassium permanganate ($KMnO_4$, AR) were obtained from Aladdin Co., Ltd. Hydrogen peroxide (H_2O_2, GR, 30%), acetic acid,

sulfuric acid (H_2SO_4, 98%, GR) and hydrochloric acid (HCl, 36.5 wt%, AR) were purchased from Sino-Pharm Group Co., Ltd. Chitosan (CS) with 80~95% deacetylation degree and 50-800 cP viscosity was purchased from Sigma-Aldrich Chemical Reagent Co., Ltd. CS was passed through sodium hydroxide solution (50 wt%) to alkalize 24 h before use and stored at -20 °C, according to procedures described in the literature[51]. Millipore water was used in all experiments and other reagents were used as received.

2.2 Synthesis of Hydroxyethyl Chitosan (HECS)

HECS was synthesized by using an improved method according to previous report[43,45]. First, 130 mL of isopropanol was added to the alkalized chitosan solution, the temperature was raised to 80 °C, stirred for around 40 minutes, after then, cooled to room temperature (RT). Then, the mixed solution of isopropanol (30 mL) and 2-chloroethanol (18 mL) was added and stirred for 6 h. Next, pH was adjusted to 7 by using hydrochloric acid solution, the solution was washed with anhydrous ethanol, followed by dialysis and freeze-drying under vacuum to acquire the pure product.

2.3 Synthesis of the Dithiol-modified Graphene Oxide (t-GO)

Graphene oxide (GO) was first synthesized, and GO was prepared via the method by Marcano et al[52], following reformative Hummers' method to implement[53] (Supplementary Information). With DTT modification of graphene oxide (t-GO) was prepared effectively through reactions between the thiol end groups with the functional groups on GO nanosheets[49]. GO nanosheets (5.0 mg) in distilled water (5.0 mL) was ultrasound-treated for 3 h and the stock solution was prepared. Then, DTT

(580 μL) was added under the continuous magnetic stirring at 90 °C last for 30 minutes, and the homogeneous black dispersion solution was obtained.

2.4 Synthesis of pNiPAM Polymer

The pNiPAM polymer with unique temperature sensitivity discoloration was prepared by a markedly simple free-radical polymerization method[54]. The whole reaction system was carried out in an oil bath under nitrogen atmosphere. After NiPAM (1.5842 g) in distilled (DI) water (50 mL) was added, O_2 in the solution was removed by N_2 bubbling stirring and lasting for 40 minutes. Then, crosslinking agent MBA (0.0324 g), initiator APS (0.0319 g) and catalyst SBS (0.0146 g) were added successively. Next, triggering the polymerization reaction by gradually raising up the temperature, the solution was changed from clarification to homogeneous milk white visibly. With vigorous magnetic stirring at 65 °C, white suspended precipitate was obtained. After 6 h, the reaction will be terminated by cooling down to RT. The obtained products were dialyzed for 1 week and the unreactive monomers were removed by changing distilled water twice a day.

2.5 Preparation of pNiPAM/HECS (pNH) Hydrogels

To fabricate the pNiPAM/HECS/t-GO (pNHG) composite hydrogels, giving priority to crosslinked pNH hydrogels were synthesized by *in situ* free radical copolymerization of NiPAM and HECS in aqueous suspension with MBA as cross-linker, using surfactant free emulsion polymerization (SFEP) method[9]. First, HECS (0.1320 g) was dissolved in deionized water (50.0 mL) with trace of acetic acid under magnetic stirring for 30 minutes to make sure that HECS was dissolved

completely, followed by addition of NiPAM (0.1584 g). After purging with nitrogen gas for 40 min to eliminate oxygen, the MBA (0.0324 g), APS (0.0319 g) and SBS (0.0146 g) were added into the solution successively. The temperature was raised up to 65 °C and the polymerization reaction was allowed to continue under N_2 atmosphere at a constant stirring. After 6 h, the reaction was terminated by cooling down to RT. The samples were freeze-dried before further use.

2.6 Preparation of pNiPAM/HECS/t-GO (pNHG) Hydrogels

Next, the incorporation of t-GO nanosheets into pNH hydrogels to further prepare the nanocomposite pNHG hydrogels, the mixed solution consisting of pNH (0.6 g), deionized water (3.9 mL) and t-GO nanosheets (600 µL) was stirred in an ice-water bath for 5h. When t-GO nanosheets was added, the solubility of the solution increased significantly and became smooth, changing from slightly yellow to light brown. Eventually, the hydrogels were freeze-dried before characterizations.

2.7 Transmission Electron Microscopy (TEM)

The morphology of GO and t-GO nanosheets was investigated using Transmission electron microscopy (TEM, Tecnai G2 F20) operating at 200 kV. For TEM sample preparation, GO and t-GO nanosheets were ultrasonically dispersed in distilled water, respectively, and a drop of the suspension was dropped onto a carbon-coated copper mesh and dried at RT.

2.8 X-ray Photoelectron Spectroscopy Analyzer (XPS)

The X-ray photoelectron spectroscopy analyzer (XPS, K-Alpha 0.05 eV, Thermo Scientific) was used to test the processed samples to obtain the elements composition

t-GO nanosheets.

2.9 Fourier-transform Infrared Spectroscopy (FT-IR)

Fourier-transform infrared spectroscopy (FT-IR, ThermoFisher, Nicolelis5) spectra of the obtained HECS, and the moveable liquid hydrogels were recorded. The FT-IR spectra range was between 4000 and 500 cm^{-1}, with using attenuated total reflectance (ATR) technique.

2.10 Scanning Electron Microscopy (SEM)

The samples (pNH and pNHG hydrogels) for SEM test were pretreated by freeze-drying. The morphology of the freeze-dried specimens was observed by using scanning electron microscopy (SEM, Hitachi, Japan, Model S-4800).

2.11 Nuclear Magnetic Resonance (NMR)

The proton nuclear magnetic resonance (^{1}H NMR 600 MHz NMR spectrometer, JEOL ECZ600R/S3) were used to confirm the successful synthesis of HECS and pNiPAM polymer.

2.12 Differential Scanning Calorimeter (DSC)

The sample for differential scanning calorimeter (DSC) analysis was pretreated by freeze-drying. The VPTT measurements of the freeze-dried samples were carried out on a TAQ100 DSC under a nitrogen atmosphere, at a heating rate of 10 °C min^{-1} from 10 to 250 °C. To prevent weight loss, sealing measurement is used instead of atmospheric pressure measurement

2.13 Spectrophotometric Measurement

The phase transition of the nanocomposites in aqueous solution was determined

utilizing the spectrophotometric method. Briefly, ~300 µL each of the nanocomposite solutions were filled in the wells of 96-well polystyrene plates. The plates were read on a temperature-controlled Spectramax M5 microplate reader (Molecular Devices, Sunnyvale, CA, USA) at 480 nm. The sol-gel transition was determined by slowly heating with the change rate of 1 °C/min from 25 °C to 42 °C. The samples were equilibrated for 10 min at temperature.

2.14 Rheological Measurement

American TA Instrument DHR rheometer was used to investigate the rheological behavior of the hydrogels, which with parallel plate geometry (40 mm in diameter). The storage modulus (G') and the loss modulus (G") at optimum gel temperature (strain of 1% and frequency of 1 Hz) were monitored as a function of time in the process of hydrogel formation. To measure the sol-to-gel transition temperature, the composite hydrogel was took out from 4 °C and then about 2.0 mL solution was quickly added onto the plate with a settled temperature of 10 °C a to keep the sol state. Afterwards, the temperature ramp was conducted at a constant frequency of 1 Hz and strain of 1.0% automated controlled by the machine. The gelation kinetics of different component hydrogels experiments was conducted at a constant frequency of 1 Hz and strain of 1.0% under the certain transformation temperature respectively. The composite hydrogel about 2.0 mL solution was quickly added onto the plate with a settled temperature of 10 °C to keep the sol state, and then the time measurement was started within 30 minutes under maintain the determinate transformation temperature. Above all, the properties of hydrogel were tested within the linear viscoelastic range.

2.15 Cell Culture

The human bone mesenchymal stem cells (hBMSCs, Normal, Human, ATCC@PCS-500-012™) were cultivated using DMEM complete medium (DMEM basic medium with 10% serum and 1% mixture of streptomycin and penicillin) in 37 °C incubator containing 5% CO_2. The primary cells were thawed in a constant temperature water bath at 37 °C, centrifuged and cultured in DMEM complete culture medium. The cells at passage 5 was used for the following experiments.

2.16 In vitro Cell Viability

The cell viability of hBMSCs in pNHG hydrogels was quantitatively investigated by Cell Counting Kit-8 (CCK-8). Ulteriorly, the biocompatibility of the pNHG hydrogels was demonstrated by DAPI, phalloidin staining the nucleus and cytoskeleton, respectively. Finally, the cells were washed twice with PBS and observed using the Confocal laser scanning microscope (CLSM).

2.17 Cells-laden pNHG Hydrogels Fabrication

The pNHG composite hydrogels after freeze-drying were put into the culture dish and culture solution was added, making it a sol state at RT. The hBMSCs were digested and DMEM complete medium was added. Then, the pNHG solution was added in the cell suspension, after mixing well, the cells were placed in an incubator of 37 °C and the growth status recorded and the culture medium changed regularly. Finally, the cells in the hydrogels were observed using CLSM.

2.18 In vitro experiments

8-week-old Sprague–Dawley (SD) rats (330–350 g, SPF) were anesthetized with

ethyl ether. Then, 1 mL of pNHG solution composited with hBMSCs was subcutaneously injected into neck of rats by a syringe. All animals were treated in accordance with the “Principles of Laboratory Animal Care” (NIH publication #85-23, revised 1985). At day 1, 7, 14 and 28 days, the animals were sacrificed, and the injection site was carefully cut open. The surrounding tissues of hydrogel were surgically removed and histologically processed using hematoxylin-eosin (HE) and Masson, and Safranin stains for the examination of inflammatory responses of synthesized polymers in rats.

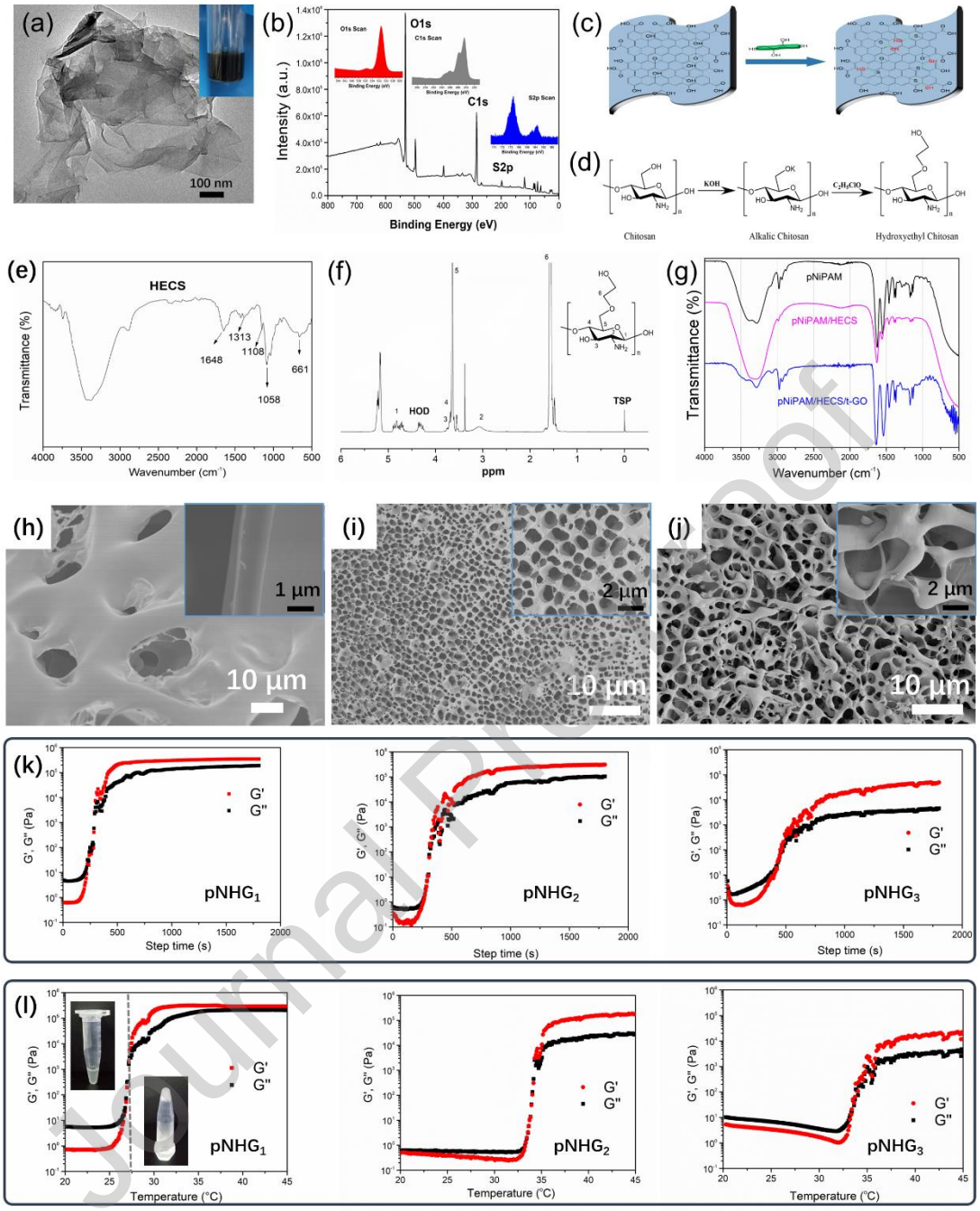

Figure 2. (a) TEM image of t-GO nanosheets, the inset at the right-top corner is the photograph of t-GO dispersed in water uniformly, (b) XPS spectra of t-GO nanosheets, including C1s, O1s, and S2p scannings, (c) schematic illustration of chemical interaction between DTT and GO nanosheets to synsthesize t-GO nanosheets. (d) The synthetic scheme of HECS, (e) FT-IR spectrum and (f) ^{1}H NMR spectrum of HECS. (g) FT-IR spectra of pNiPAM polymer, pNiPAM/HECS (pNH), and

pNHG hydrogels. SEM images of (h) $pNHG_1$, (i) $pNHG_2$, and (j) $pNHG_3$ hydrogels after freeze-dried, SEM images inserted at the right-top of images (h-j) were enlarged at a higher magnification. Rheological analysis of pNHG hydrogels (k) over time and (l) temperature, the gelation time was tested under 37 °C, and the photos inserted at the first figure of (l) showed that pNHG solution was transferred to hydrogel state while the temperature above the crossover point.

3. Results and discussion

GO nanosheets were synthesized using a modified Hummers' method [55,56]. Our previous study confirmed that GO flake thickness was approximately 1.25 nm, composed of two stacked individual monatomic GO layers [50]. After DTT modified on GO nanosheets, the thickness of t-GO nanosheets was increased to around 2 nm, speculating that more layers were stacked together (**Figure 2a**). The obtained t-GO nanosheets could be uniformly dispersed in water. The FT-IR spectra of GO and t-GO (**Figure S1**) confirmed that the formation of C-S bonds (1035 cm^{-1}) and S-H bonds (730 cm^{-1}) in t-GO nanosheets, and the formation of C-S bonds between DTT and GO nanosheets was also identified via XPS analysis (**Figure 2b** and **Figure S2**)[56]. Due to the oxygen functionalities inserted on GO nanosheets, such as hydroxyl groups, carboxylic acids, and epoxides [57], DTT molecules are connected via C-S bonds, and the possible graft mechanism is illustrated in **Figure 2c** and **Figure S3** [58].

HECS was synthesized via the reaction of alkalified chitosan with 2-chloroethanol (**Figure 2d**) [45,59]. The FT-IR spectrum of HECS was shown in **Figure 2e**. The detected -CH_2- bending vibration at 1313 cm^{-1}, stretching vibration of C-O-C

at 1108 cm^{-1}, and C-O stretching vibration of C-O at 1058 cm^{-1} confirmed that 2-chloroethanol reacted with chitosan successfully. The ^{1}H NMR analysis of HECS (**Figure 2f**) was performed, the multiplets at δ values of 3.1-4.0 (H-2, H-3, H-4, H-5, and H-6) corresponded to the ring methine protons, and the signal at δ = 3.6 was assigned to the methylene protons. At the same time, the pNiPAM polymer could be successfully synthesized by the free-radical polymerization method (**Figure S4**) [54]. After then, HECS was dissolved in deionized water, acetic acid was added to ensure the complete dissolution of HECS, and the monomer of NiPAM was added under nitrogen gas to synthesize pNiPAM/HECS (pNH) composite. The obtained pNH was melt in an ice-water bath, and the white liquid of pNH was obtained after the rotary evaporated. Then, the t-GO nanosheets were composited into pNH, and the light-yellow liquid was displayed (**Figure S5**). The FT-IR spectra of pNiPAM polymer, pNH nanocomposite, and pNHG nanocomposite were shown in **Figure 2g**. For pNiPAM, peaks at 1631 cm^{-1}, 1559 cm^{-1}, and 1395 cm^{-1} corresponded to amide I, amide II, and methyl groups, respectively [60]. For pNH, the intensity of the O-H group at 3430 cm^{-1} had increased compared to pNiPAM, and the peak at 1154 cm^{-1} was assigned to the asymmetric stretching of glycosidic linkage joining two monosaccharides of HECS (**Figure S6**) [15]. Compared with pNiPAM polymer and pNH composite, the multi-peaks from 600-500 cm^{-1} appeared in pNHG nanocomposite, and peaks at 2929 cm^{-1} and 2856 cm^{-1} assigned to methylene groups were intensified as well. Zuo *et al.* [61] confirmed that GO could be evenly dispersed within CS matrix via the formation of amide linkages between GO's carboxylic acid

groups and CS's amine groups. Here, the solubility of pNHG nanocomposite in water was significantly improved compared to pNiPAM/HECS/GO, such phenomenon could be explained by the increased hydrogen bonds between polymer pNiPAM and HECS, and t-GO nanosheets[62], and the performance of improved GO solubility could expand its applications in drug delivery and cell loading[63]. In this work, the cell dispersion and cell viability in pNHG hydrogels was enhanced due to the improvement of solubility of pNHG in water, such enhanced biological properties could facilitate the potential use of cell-laden pNHG hydrogels as bio-inks in 3D bioprinting, such as extrusion bioprinting[64].

Here, three types of pNHG hydrogels were fabricated (**Table S1**). After freeze-drying, the white solid of pNHG (**Figure S7**) was dissolved in cold water (0-20 °C, around 0.045 g/mL), resulting in a white uniform solution, different from the solution of pNH in which the sedimentation was observed due to the aggregation of GO nanosheets. While increasing the temperature to around 30 °C, the pNHG solution gradually transferred to a hydrogel state. The morphology of pNHG hydrogels after freeze-drying was characterized by SEM images (**Figure 2h-j**). All pNHG hydrogels samples showed an apparent porous structure after freeze-drying, and t-GO nanosheets were dispersed uniformly in the polymer networks without phase separation. Compared to the freeze-dried pNH hydrogels, pNHG hydrogels displayed a larger pore size (**Figure S8**), which facilitated the cell proliferation due to the sufficient nutrition supply[65]. In addition, the TEM analysis showed that the t-GO nanosheets were connected with the surrounding polymer fibers (**Figure S9**). The size

and distribution of the pores influence the cell growth and mass transfer of the cell-laden matrix. Especially, $pNHG_2$ has shown homogeneously distributed porous microstructure.

Next, the low critical solution temperature (LCST) evaluating the sol-to-gel transfer of pNHG hydrogel was investigated in the temperature range of 20-45 °C using a rheometer [66] and a spectrophotometer (480 nm) [67]. Due to the interaction between the pNiPAM, HECS, and t-GO nanosheets, and self-assembly of hydrophobic and hydrophilic moieties in pNHG occurred with the increase of temperature, which resulted in the sol-gel transfer (**Figure 1b**). The gelatinous behaviour and mechanical properties of pNHG hydrogel could be characterized by rheological characterization. The storage and loss moduli in terms of time and temperature for pNHG hydrogels were shown in **Figure 2k and 2l**. The gelation time and LCST were both confirmed based on the crossover point of the storage moduli (G') and loss moduli (G'') [66]. The gelation time for $pNHG_1$, $pNHG_2$, and $pNHG_3$ were 230 s, 309 s, and 400 s, respectively, and the LCST for $pNHG_1$, $pNHG_2$, and $pNHG_3$ were 27.1 °C, 34.2 °C and 34.1 °C, respectively, and the obtained results were consistent with data measured via spectrophotometer method (**Figure S10**). Compared with pNH hydrogels (**Figure S11**), the LCST of pNHG hydrogels were not changed; however, the sol-gel transfer process became faster, which was attributed to the formation of t-GO nanosheets network interpenetrated in the polymer of pNiPAM and HECS networks, and such inorganic network structure resulted in the further increase of storage moduli after the hydrogel formation [49]. In addition, the transition

from a clear transparent liquid to an opaque hydrogel could be observed by a simple test tube inverting method, as shown in photos inserted in **Figure 2l** [68,69].

Furthermore, the pNHG has a temperature-reversible property, and due to the weak reversible hydrogen bonds within the hydrogel matrix, it becomes transparent liquid again when it is cooled. The relationship between the LCST and solution concentration of composite was also investigated and exhibited that LCST had a slight increase with the increase of nanocomposite weight in water. According to the DSC results (**Figure S12**), the coil-globule volume phase transition temperature (VPTT) for $pNHG_1$, $pNHG_2$, and $pNHG_3$ were 33.97, 33.02 and 34.11 °C, respectively. Also, the endotherm peaks that appeared at 68-93 °C corresponded to the destruction of hydrogen bonds. The unique interpenetrating structure and hydrogen bonding played critical roles in not only enhancing the mechanical property of pNHG hydrogels, but also the fine regulation of LCST.

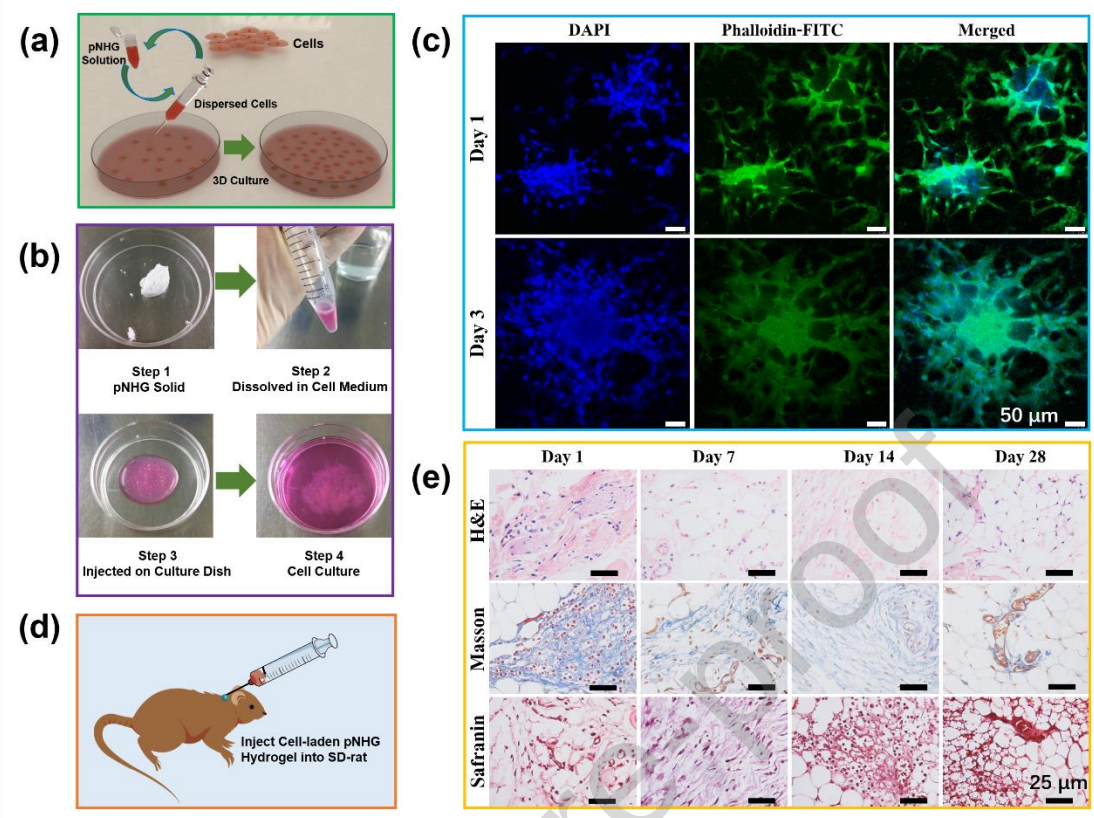

Figure 3. (a) The illustration of cell-laden pNHG hydrogel preparation. (b) the white pNHG solid powder is dissolved in cell solution (around 20 °C) first, and the cell-loaded solution is transferred to Petri plate, then the Petri plate is put in cell incubator with 95% air and 5% CO_2 at 37 °C, once the cell-laden hydrogel is formed, more cell medium is added for further cell growth. (c) Fluorescent images of hBMSCs encapsulated in $pNHG_2$ hydrogels over days, the cells are stained with DAPI (blue) and Phalloidin-FITC (green). (d) the illustration of hBMSCs-laden $pNHG_2$ hydrogel injected in the neck of SD rat. (e) Optical micrographs of H&E, Masson, and Safranin staining slices of surrounding tissues after injection of hBMSCs-laden $pNHG_2$ hydrogel subcutaneously over days.

After that, the cytocompatibility of pNH and pNHG hydrogels was investigated by culturing with human bone mesenchymal stem cells (hBMSCs). CCK-8 data

confirmed that the cell viability of hBMSCs increased on both pNH and pNHG hydrogels over days, and the addition of t-GO nanosheets improved the cell viability inside the hydrogels. The reinforced pNHG hydrogel provided a suitable 3D microenvironment for cell growth compared to the pNH hydrogel (**Figure S13** and **Figure S14**). The cells in culturing medium were added in pNHG nanocomposites solution and dispersed homogeneously, then cell-laden hydrogel was fabricated by increasing temperature above 34 °C (**Figure 3a** and **3b**). In addition, the prepared cell-laden pNHG hydrogel could be injected on the cultring dish using a injection syringe, the excellent extrudability and filament uniformity were observed, confirming the potentials of hydrogels as bioink for 3D extrusion bioprinting[64,70,71]. hBMSCs cells adhered and proliferated into pNHG hydrogels over days (**Figure 3c**). Even increasing the number of hBMSCs cells encapsulated in the pNHG hydrogels still displayed a slight increase of cell viability; however, the relative cell viability decreased (**Figure S15**). Moreover, different types of cells encapsulated in hydrogels had no significant differences in cell viability (**Figure S16**). Usually, cells pool in the hydrogel and first recognize the adhesion motifs, such as Arg-Gly-Asp (RGD) peptide, fibronectin, and laminin, and then settle down, extend, and migrate along with the networks [72,73]. The reinforced pNHG hydrogels with interpenetrating polymer networks provided a suitable 3D microenvironment for cell adherence and proliferation (**Figure S17** and **Figure S18**). Lastly, the *in vivo* sol-gel formation of pNHG solution with hBMSCs was evaluated by injecting into the neck of Sprague-Dawley (SD) rats (330-350 g) and the gels formed after the injection (**Figure**

3d). On day 1, 7, 14 and 28, the injected hydrogels were taken out and further histologically processed using hematoxylin-eosin (HE), Masson and Safranin stains to investigate the inflammatory responses. Many inflammatory cells, including lymphocytes and macrophages, were observed, and such cell number decreased over days. On day 28, the newly formed blood vessels were observed (**Figure 3e**). The results confirmed that the fabricated hBMSCs-laden pNHG hydrogels had excellent histocompatibility and angiogenic functions for further biomedical applications.

4. Conclusion

In summary, the cytocompatible temperature-responsive Pnhg hydrogel for cell encapsulation was developed using pNiPAM, HECS and t-GO nanosheets. We could regulate the LCST by varying the weight ratio of pNiPAM/HECS/t-GO and could encapsulate hBMSCs in the hydrogel at a low temperature around 20 ºC. The results highlighted that the incorporation of t-GO nanosheets improved the cell viability inside the hydrogels, and the reinforced pNHG hydrogel provided a suitable 3D microenvironment for cell growth.

Author Contributions

The manuscript was written through the contributions of all authors. All authors have approved the final version of the manuscript.

Acknowledgements

The authors acknowledge support from the National Natural Science Foundation of China (31700840). In addition, LN acknowledges the encouragement and support from Yang Yuan. Finally, the authors acknowledge the help from Prof Lingling Wang, Prof. Qiuju Zhou, Dr. Zongwen Zhang, and Dr. Dongli Xu, in the Analysis & Testing Center of XYNU.

Conflicts of interest

The authors declare no competing financial interest.

References

1. Esch, E. W.*, et al.*, *Nat Rev Drug Discov* (2015) **14** (4), 248
2. Talebian, S.*, et al.*, *Adv Sci* (2019) **6** (16), 1801664
3. Malda, J.*, et al.*, *Adv Mater* (2013) **25** (36), 5011
4. Huang, S. T.*, et al.*, *J Appl Polym Sci* (2015) **132** (9)
5. Ahadian, S.*, et al.*, *Chem Eng Prog* (2018) **114** (5), 56
6. Zhang, Y. S., and Khademhosseini, A., *Science* (2017) **356** (6337)
7. Chen, D.*, et al.*, *Mater Lett* (2018) **229**, 138
8. Deka, S. R.*, et al.*, *Nanoscale* (2011) **3** (2), 619
9. Echeverria, C.*, et al.*, *Mater Design* (2015) **86**, 745
10. Hoshino, Y.*, et al.*, *Adv Mater* (2014) **26** (22), 3718
11. Huang, N.*, et al.*, *Chemphyschem* (2014) **15** (9), 1785
12. Motornov, M.*, et al.*, *Progress in Polymer Science* (2010) **35** (1-2), 174

13. Perez-Alvarez, L., *et al.*, *Macromol Chem Phys* (2009) **210** (6), 467

14. Si, T. B., *et al.*, *React Funct Polym* (2011) **71** (7), 728

15. Sun, M. M., *et al.*, *Eur Polym J* (2015) **66**, 569

16. Xulu, P. M., *et al.*, *Macromolecules* (2000) **33** (5), 1716

17. Yu, J. W., *et al.*, *Polymer Chemistry* (2016) **7** (1), 36

18. Zhao, C. S., *et al.*, *Progress in Polymer Science* (2011) **36** (11), 1499

19. Zhuang, J. M., *et al.*, *Chem Soc Rev* (2013) **42** (17), 7421

20. Tang, J. D., *et al.*, *J Am Chem Soc* (2019) **141** (12), 4886

21. Lue, S. J., *et al.*, *Journal of Macromolecular Science, Part B* (2011) **50** (3), 563

22. Liu, H., *et al.*, *Macromolecular Rapid Communications* (2001) **22** (9), 675

23. Haq, M. A., *et al.*, *Mat Sci Eng C-Mater* (2017) **70**, 842

24. Yang, J. L., *et al.*, *Journal of Materials Chemistry B* (2016) **4** (40), 6609

25. Li, Z. Q., *et al.*, *Soft Matter* (2012) **8** (11), 3139

26. Li, Z. Q., *et al.*, *Mat Sci Eng C-Mater* (2013) **33** (4), 1951

27. Zhang, H. J., *et al.*, *Rsc Adv* (2015) **5** (108), 89073

28. Lee, J. H., and Kim, H. W., *J Tissue Eng* (2018) **9**, 2041731418768285

29. Cavo, M., *et al.*, *Sci Rep* (2016) **6**, 35367

30. Caiazzo, M., *et al.*, *Nat Mater* (2016) **15** (3), 344

31. Qiao, Z., *et al.*, *Polymers* (2019) **11** (11)

32. Yuan, T., *et al.*, *Macromolecules* (2019) **52** (8), 3141

33. Sun, J. Y., *et al.*, *Nature* (2012) **489** (7414), 133

34. Dragan, E. S., *Chemical Engineering Journal* (2014) **243**, 572

35. Shariatinia, Z., *Adv Colloid Interfac* (2019) **263**, 131

36. Nie, L.*, et al.*, *J Biomat Sci-Polym E* (2019) **30** (17), 1636

37. Balasubramaniam, M. P.*, et al.*, *Mater Today Commun* (2020) **25**

38. Borgohain, R., and Mandal, B., *ACS Appl Mater Interfaces* (2019) **11** (45), 42616

39. Rasib, S. Z. M.*, et al.*, *Int J Biol Macromol* (2018) **108**, 367

40. Wang, L.*, et al.*, *Carbohydr Polym* (2017) **174**, 904

41. Ding, H.*, et al.*, *Advanced Healthcare Materials* **n/a** (n/a), 2000454

42. Nanaki, S. G.*, et al.*, *Carbohyd Polym* (2012) **87** (2), 1286

43. Shao, K.*, et al.*, *J Ocean U China* (2015) **14** (4), 703

44. Wang, H. J.*, et al.*, *Cancer Cell Int* (2017) **17**

45. Nie, L.*, et al.*, *Acs Omega* (2020) **5** (19), 10948

46. Nie, L.*, et al.*, *Mater Lett* (2020) **280**

47. Liu, C. Y.*, et al.*, *Polymers* (2018) **10** (8)

48. Dai, H. J.*, et al.*, *Carbohyd Polym* (2018) **185**, 1

49. Du, G. L.*, et al.*, *Acs Applied Materials & Interfaces* (2015) **7** (5), 3003

50. Nie, L.*, et al.*, *Sn Applied Sciences* (2019) **1** (6)

51. Wang, Y. P.*, et al.*, *Carbohydrate Polymers* (2017) **167**, 44

52. Marcano, D. C.*, et al.*, *Acs Nano* (2010) **4** (8), 4806

53. Ma, X. M.*, et al.*, *European Polymer Journal* (2013) **49** (2), 389

54. Marques, N. D.*, et al.*, *Journal of Applied Polymer Science* (2013) **129** (1), 334

55. Nie, H. B.*, et al.*, *Materials* (2018) **11** (4)

56. Nie, L.*, et al.*, *Mater Lett* (2020) **261**

57. Chua, C. K., *et al.*, *Chem-Eur J* (2012) **18** (42), 13453

58. Stergiou, A., *et al.*, *Progress in Materials Science* (2020) **114**, 100683

59. Luo, B., *et al.*, *J Appl Polym Sci* (2012) **125** (S2), E125

60. Jaiswal, M. K., *et al.*, *Colloid Surface B* (2010) **81** (1), 185

61. Zuo, P. P., *et al.*, *Chem Cent J* (2013) **7**

62. Neklyudov, V. V., *et al.*, *Phys Chem Chem Phys* (2017) **19** (26), 17000

63. Liu, J. Q., *et al.*, *Acta Biomater* (2013) **9** (12), 9243

64. Mirzaei, M., *et al.*, *Bioengineering-Basel* (2021) **8** (4)

65. Seidel, J., *et al.*, *Biofabrication* (2017) **9** (4)

66. Jia, Z. F., *et al.*, *Mat Sci Eng C-Mater* (2019) **99**, 541

67. Durkut, S., *International Journal of Polymeric Materials and Polymeric Biomaterials* (2019) **68** (17), 1034

68. Zou, P., *et al.*, *J Mater Chem* (2012) **22** (13), 6316

69. Nie, L., *et al.*, *Journal of Materials Science-Materials in Medicine* (2013) **24** (3), 689

70. Shavandi, A., *et al.*, *Advanced Healthcare Materials* (2020) **9** (24)

71. Han, Y. T., *et al.*, *Crystals* (2021) **11** (4)

72. Vega, S. L., *et al.*, *Nat Commun* (2018) **9**

73. Kessler, L., *et al.*, *J Tissue Eng* (2017) **8**, 2041731417744157

CRediT authorship contribution statement

Lei Nie: Conceptualization, Methodology, Software, Validation, Formal analysis, Investigation, Data Curation, Writing - Original Draft, Writing - Reviewing and

Editing, Supervision, Project administration, Funding acquisition. **Jie Li**: Methodology, Software, Validation, Formal analysis, Investigation, Data Curation, Writing - Original Draft. **Guoqi Lu**: Methodology, Investigation, Data Curation. **Xiaoyan Wei**: Software, Formal analysis, Writing - Reviewing and Editing. **Yaling Deng**: Software, Validation, Formal analysis. **Shuang Liu**: Formal analysis, Data Curation. **Shengping Zhong**: Methodology, Software. **Qimin Shi**: Methodology, Software. **Yi Sun**: Methodology, Software. **Constantinus Politis**: Methodology, Software. **Lihong Fan**: Supervision, Writing - Reviewing and Editing. **Oseweuba Valentine Okoro**: Supervision, Writing - Reviewing and Editing. **Amin Shavandi:** Writing - Original Draft, Writing - Reviewing and Editing.

Declaration of interests

☒ The authors declare that they have no known competing financial interests or personal relationships that could have appeared to influence the work reported in this paper.

☐The authors declare the following financial interests/personal relationships which may be considered as potential competing interests:

No potential conflicts of financial interests/personal relationships were reported by all-authors.

Graphical abstract